

Preparation of Polyaniline Multi-wall Carbon Nanotubes Nanocomposites Films/Discs and Characterization of their Electrical, Mechanical and Damping Properties

¹ Weiwei LIN, ² Xiangxing KONG, ¹ Cesar LEVY

¹ Department of Mechanical and Materials Engineering,
Florida International University, Miami, FL 33162, USA

² Center for Biosignatures Discovery Automation, The Biodesign Institute
Arizona State University, Tempe, AZ 85287, USA

¹ Tel.: +1-305-348-3643, fax: +1-305-348-1932

¹ E-mail: levyez@fiu.edu

Received: 31 March 2015 / Accepted: 27 March 2015 / Published: 30 April 2015

Abstract: The purpose of this research was to create a sensor-actuator that could sense strain and also act similar to constrained viscoelastic material without corresponding weight addition. Frit compression method was first used to make controlled thickness of polyaniline/multi-wall carbon nanotube (PANI/MWCNT) nanocomposite films/discs. MWCNT was found to enhance both the electrical conductivity and the thermal stability properties of the nanocomposite films, and the PANI increased the Young's modulus and hardness of the films/discs as evidenced by the nanoindentation test. Simultaneous DSC-TGA measurements showed that the PANI/22%MWCNT nanocomposites improved their thermal stability by about 50 °C compared with their pure components. Cantilever beam free vibration tests were adopted to characterize the sample damping properties. It was found that location of the sample vis-à-vis the location of the cantilever beam's fixed support played a very important part in the damping ratio, as expected. Preliminary tests showed that the damping ratio of PANI/11%MWCNT was 0.00656 when the aluminum beam was clamped to the free, uncovered end. However, the damping ratio nearly tripled when the beam was clamped at the PANI/MWCNT covered end. By covering both sides of aluminum beam with the sample, the damping ratio reached a value of 0.072, which is 18.85 times higher than for the single sided coverage. *Copyright © 2015 IFSA Publishing, S. L.*

Keywords: PANI/MWCNT, Frit compression, Electrical properties, Mechanical properties, Damping properties.

1. Introduction

Structural-borne vibration is one of the key issues for army combat vehicles, gun platforms and the gun barrels. Successful vibration suppression improves the accuracy of surveillance, targeting and firing. The prospect of Polymer/MWCNT composites serving as damping materials has been studied broadly in the

recent past [1-6]. The purpose of this investigation is to verify that such a fabricated composite can act both as a sensor and a damper.

Polyaniline (PANI) is one of the most studied conducting polymers of the past 50 years, and it is the cheapest one among its conducting polymer family. Carbon nanotubes (CNT) have drawn much attention since their discovery in 1991 [7] because of their

unique mechanical and electronic properties. Up to now, most polyaniline/carbon nanotube (PANI/CNT) nanocomposites materials obtained by the chemical methods were in the powder form [8, 9]. Though some papers stated that binding materials were used when making PANI/CNT nanocomposites [8, 10, 11], the binding materials were thought to deteriorate the chemical or mechanical properties of PANI/CNT nanocomposites films. Flexible carbon nanotube/polyaniline films were fabricated by immersing the multi-wall carbon nanotube (MWCNT) network template into the *in situ* aniline polymerization solution [12]. However, their electrical, electrochemical or mechanical properties could not be mostly optimized due to their heterogeneous nature. Furthermore, because it is difficult to control the thickness of polyaniline/multi-wall carbon nanotube (PANI/MWCNT) nanocomposites films, there are very few papers reporting their damping properties.

Frit compression is a technique used to fabricate buckypaper and buckydiscs from a suspension of carbon nanotubes in a solvent [13]. The Whitby research group [14] first used the frit compression method to successfully fabricate MWCNT buckypaper/buckydiscs. Buckypaper has been created using MWCNT in a water suspension with surfactant added technique [15]. Compared with surfactant casting or acid oxidation filtration methods, the buckypaper/buckydiscs created by the frit compression method avoids any surfactant or surface modification techniques. Also, the distribution of CNT in solvent doesn't need to be a thermally stable suspension. A general dispersion of CNT in solvent will keep the nanotubes between the frits rather than allowing them to pass through the frits. This methodology rapidly speeds up the casting process and the solvent can be fully recovered, making it an efficient method to fabricate polymer composites films/discs.

Herein, the frit compression method is introduced to fabricate PANI/MWCNT nanocomposite films/discs. The thickness of these films/discs can also be controlled. The properties of electrical resistance and thermal stability of these films/discs are characterized and the mechanical properties, such as Young's modulus and hardness of the nanocomposite films/discs, are discussed. Furthermore, their preliminary damping properties are evaluated.

2. Experimental Sections

2.1. Surface Treatment of MWCNT

Two kinds of surface treatment of MWCNT were carried out, dry heat treatment and mixture acid oxidation to purify MWCNT and form ketone and acid groups. The experimental details are described below:

Dry heat treatment of MWCNT. Eight grams of MWCNT was spread equally into the bottom of a 2×4 cm ceramic bowl. The bowl was put into a muffle furnace for 80 minutes with the temperature of 450 °C for the refinement. Fig. 1 shows the heat graph of the muffle furnace.

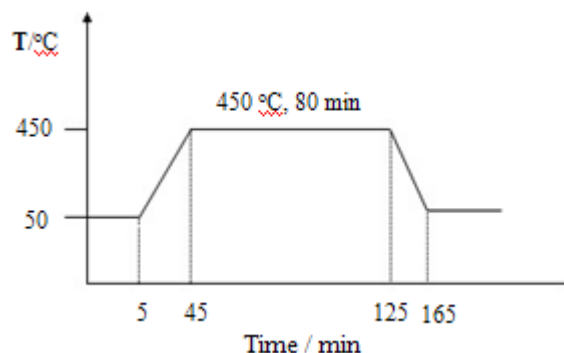


Fig. 1. The dry heat treatment processing of MWCNT.

Chemical modification of MWCNT. After heat treatment, a mixed acid solution ($\text{H}_2\text{SO}_4 : \text{HNO}_3 = 3:1$) treatment under supersonic bath was used to improve the MWNT purity by removing metal catalyst impurities [16], and to improve interfacial adhesion with polymer matrix by surface oxidation of the MWCNT to form ketone and acid groups. A large amount of distilled water was added to the MWCNT suspension. After cooling down, the suspension was added into centrifuge tubes and centrifuged at 4000 rpm for 10 min. The black MWCNT was precipitated to the bottom of the centrifuge tube. The top acid solution was safely discarded and the precipitate of MWCNT remained. The MWCNT precipitate was washed with distilled water at least five times to reach a $\text{PH} \approx 7$. Its neutralization was checked with pH measurement paper. The washed MWCNTs were dried in vacuum at 60 °C for more than 12 hrs.

2.2. In Situ Synthesizing of PANI/MWCNT Nanocomposites

Aniline was distilled under reduced pressure prior to use. PANI/MWCNT composite was prepared by *in situ* polymerization. The procedures are briefly described as follows (Table 1):

Table 1. Synthesizing different components of PANI/MWCNT composites and its control.

	MWCNT (mg)	Aniline (g)	APS (g)
Pure PANI	0	1.445	1.163
PANI/11% MWCNT	64.375	1.287	1.027
PANI/22% MWCNT	128.75	1.129	0.903
PANI/44% MWCNT	257.50	0.813	0.643
Pure MWCNT	513.06	0	0

64.375 mg of MWCNT were dispersed by sonication in 125 ml of 1M HCl for 30 min. 1.287 g of aniline was added and the mixture was sonicated for another 30 min. After that, 1.027 g of ammonium persulphate (APS) dissolved in 125 ml of 1 M HCl was added at once and polymerization was conducted at 0 °C with water-ice bath under sonication for 4 hrs. The precipitated products were washed with deionized water. Then PANI/11% wt MWCNT were made. Four different components of nanocomposites were synthesized by the same procedures (See Table 1).

2.3. Preparation of PANI/MWCNT, Pure PANI and Pure MWCNT Films

Three different ratios of PANI/MWCNT nanocomposites films listed in Table 1 were made by using frit compression methods. The procedure is described below.

454.54 mg of obtained PANI/MWCNT suspension was transferred into a specially built 50 ml cuboid mold (see Fig. 2), which was equipped with frits with a pore diameter of 70 μm (frits purchased from Sigma-Aldrich). In order to remove the solvent, 50 lbs of force was applied to the plungers (See Fig. 3). After the solvent was squeezed out, the frits-PANI/MWCNT sandwich with the cuboid mold was dried at 110 °C in an oven for 12 hrs. The PANI/MWCNT composite film was obtained after removing it from the cuboid mold. The pure PANI film was made by the same procedures as a control.

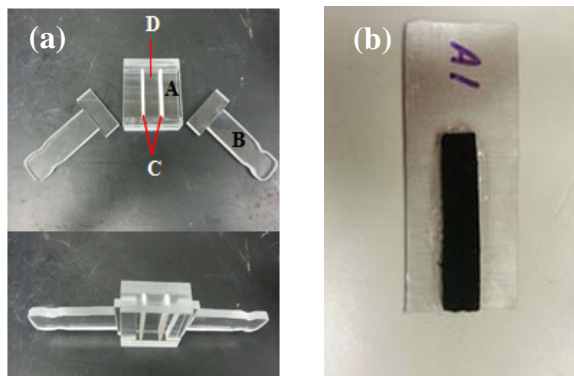


Fig. 2. The frit compression system for making nanocomposite films. (a) The frit compression system, (b) are the photo image of PANI/MWCNT nanocomposites. Inserts are A: cuboid; B: plungers; C: polypropylene frits and D: composites suspension.

The pure raw rectangular MWCNT film was prepared by the same frit compression procedure. 454.54 mg MWCNT was suspended into 3 ml deionized water, then the mixture was simply transferred into the cuboid mold to squeeze out the solvent. In a similar process as that used in preparing

the PANI/MWCNT nanocomposite films, the pure MWCNT film was obtained.

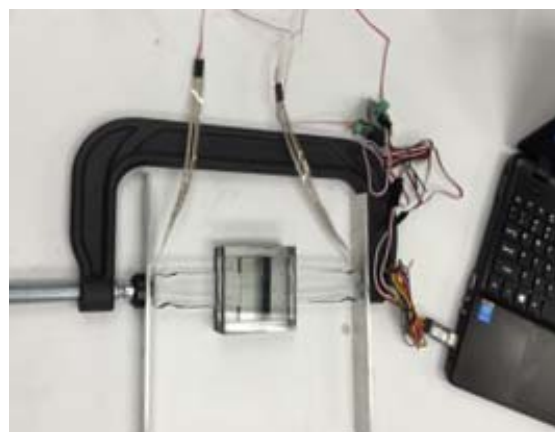


Fig. 3. Schematic image of 50 lbs force applied to plungers measured by FlexiForce adapter.

2.4. Characterization

Transmission electron microscopy (TEM) and scanning electron microscopy (SEM) were used to study their morphology properties. Two probe electrical measurement was adopted to study the electrical conductivity of different composition of PANI/MWCNT composites. Thermal stability of the PANI/MWCNT was studied by simultaneous DSC-TGA (SDT) test.

Free end vibration test method was adopted to study the damping properties of these samples. There are two different setups used to test the damping properties of the PANI/MWCNT nanocomposites: one was used to test the effect of sample size and location on the vibration damping of the beam; and, one was used to test how the sample's vibration damping capability was affected by single or double coverage of the base aluminum (Al) beam. Details were shown as the following.

2.4.1. Specimen Preparation and Purpose

Specimen for test 1: The polymer compositions of the samples used here were pure PANI, PANI/11% MWCNT, PANI/22% MWCNT, PANI/44% MWCNT and pure MWCNT. The dimensions of the samples here is 3.6 cm \times 0.8 cm \times 1.9 mm, which were bonded to the Al beams with dimension of 6 cm \times 2.5 cm \times 0.013 cm (Alloy 6061 aluminum, bought from MSC Industrial Co.) by nonconductive 3M CA100 liquid instant adhesive (See Fig. 4 (a)).

Three thin layers of adhesive were used to cover these samples to separate the samples from the environment. Each specimen was dried at room temperature for 24 hrs.

Free vibration comparisons were made by using either the sample side, #, or the uncovered side, *,

alternately, as the fixed support for the cantilever beam. The red lines shown in Fig. 4 (b) defined the locations where the beam was clamped. The unclamped side was then made to vibrate and a parameter called the damping ratio was determined.

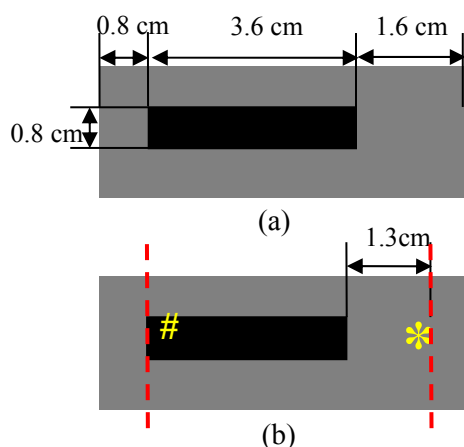


Fig. 4. (a) Size of samples, Al beams and the locations where samples were attached. (b) Locations of sample side # and free end side * where the beam was clamped.

Specimen for test 2: Two Al beams were used with thickness of 2.4 mm and width of 0.9 cm. Samples of 4 cm × 0.9 cm × 1.9 mm PANI/11% MWCNT were attached the Al base beam, one beam with single coverage and one beam with both sides covered for comparison (See Fig. 5). Three thin layers of adhesive were used to cover these samples to separate the samples from the environment. Each specimen was dried at room temperature for 24 hrs. The unclamped side was then made to vibrate and the damping ratio was determined.

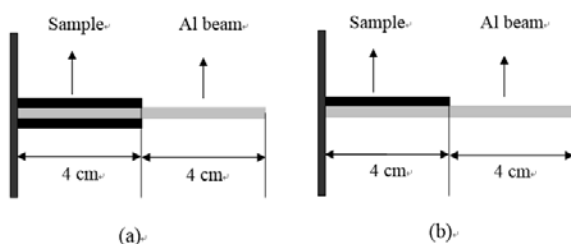


Fig. 5. (a) PANI/MWCNT sandwiched Al base beam. (b) PANI/MWCNT attached one side of Al base beam.

Specimen for test 3: Two different thicknesses of Al beams were used to evaluate thickness effects. One is thin beam with 1.25 mm thickness and the other is of 2.4 mm thickness. The width of the beam used was 0.9 cm for both beams. The dimension of the PANI/ 11 % MWCNT sample were 0.8 cm × 4 cm × 1.9 mm, which was glued onto the Al beams by adhesive. Three very thin layers of adhesive were used to cover these samples to separate the samples

from the environment. Each specimen was dried in room temperature for 24 hrs.

For each thickness beam, several tests were conducted where the clamped edge was placed at different distances (0 cm, 1.7 cm, 5.4 cm and 7.7 cm), which corresponding to redline marked as a, b, c and d (See Table 2 and Fig. 6). The unclamped side was then made to vibrate and the damping ratio was determined.

Table 2. Different thickness and distance from the clamp and the samples were tested.

Al thickness	Distance from the clamp to sample (cm)			
	2.4 mm	0	1.7	5.4
1.25 mm	0	1.7	5.4	7.7

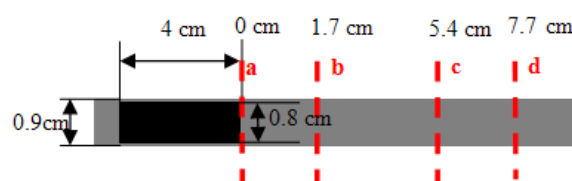


Fig. 6. Dimension of samples and locations (red lines) where the clips clamped on (a) 0 cm, (b) 1.7 cm, (c) 5.4 cm and (d) 7.7 cm away to the samples. The dimension of the sample is 4 cm × 0.8 cm × 1.9 mm. The width of the Aluminum beam is 0.9 cm.

2.4.2. Damping Test Methodology

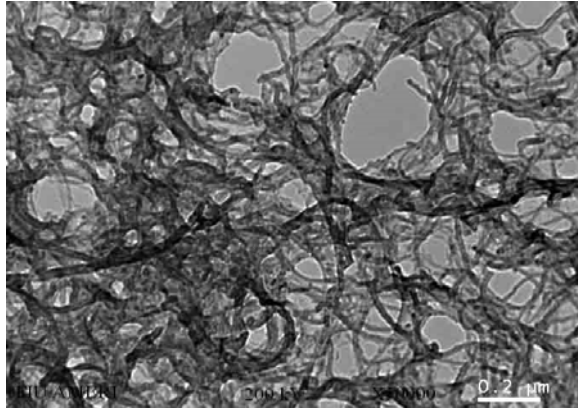
The cantilever beams of Fig. 4, 5 and 6 were given the same, small initial displacement and then released for free vibration. Free end displacements were measured by a laser vibrometer and a two channels digital oscilloscope was used display and store the signal. Five trials were made for each setup and the mean value of the damping ratio was calculated. This ratio can be related to the logarithmic decrement of consecutive maxima of end displacements and can be correlated to how much vibration energy is removed by the sample. The higher the damping ratio, the better the sample acts as a damper.

3. Results and Discussion

3.1. Morphological Characterization of the PANI/ MWCNT Film

TEM images were obtained to determine how well the MWCNT and the PANI were integrated to form a homogeneous composite. TEM images of pure MWCNT and PANI/22% MWCNT are shown in Fig. 7. The diameter of the PANI/22% MWCNT are about 60 nm (Fig. 7 (b)) while the diameter of the MWCNT are about 6-9 nm (Fig. 7 (a)). It appears

that the MWCNT nanofibers were coated with a dense PANI layer (see Fig. 7 (a)). Furthermore, these TEM images clearly displayed that the walls of PANI/MWCNT nanofibers were rougher than walls of MWCNT nanofibers. It indicated that the polymerization of PANI was at least part of nucleation growth and the MWCNT was acting like the nucleating agent, which led to a new interwoven fibrous structure (Fig. 7 (b)).



(a)

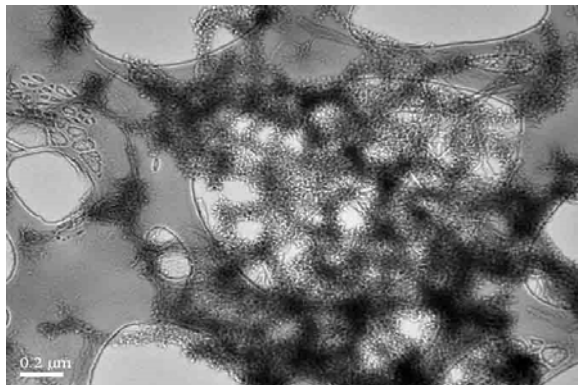


Fig. 7. TEM images of (a) pure MWCNT and (b) PANI/22% MWCNT.

SEM images were obtained to determine how well the MWCNT and the PANI were dispersed to form a homogeneous composite. SEM images of pure MWCNT, pure PANI and PANI/22% MWCNT nanocomposites films are given in Fig. 8. Compared with the random distribution of MWCNT which displayed in Fig. 8. (a) and (a'), the surface of pure PANI was much smoother (Fig. 8. (b) and (b')). The surface smoothness of PANI/22% MWCNT nanocomposite films is between the pure PANI and pure MWCNT, which indicated that while polymerization of PANI with the presence of MWCNT, the majority of MWCNT have been entrapped into the PANI films. Furthermore, the PANI/MWCNT nanocomposites showed the homogeneous coating of PANI onto the MWCNT indicating that carbon nanotubes were well dispersed

in the polymer matrix, which is constant with the TEM test results.

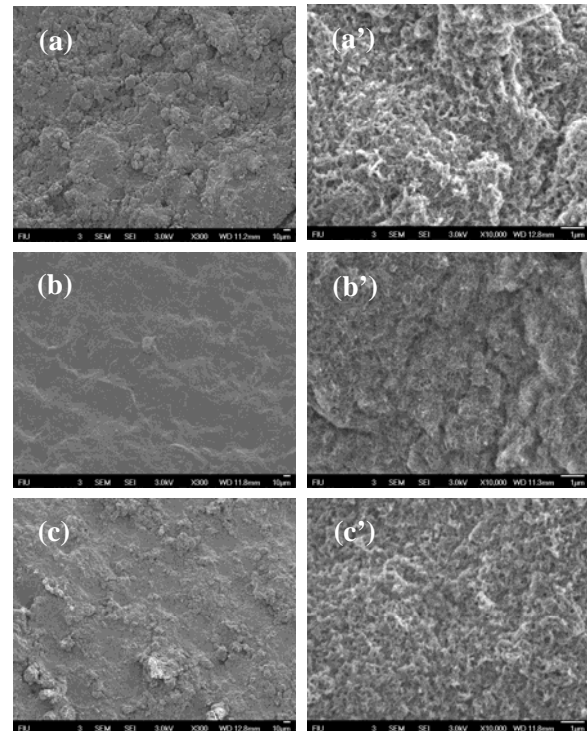


Fig. 8. SEM image of (a) pure MWCNT, (b) pure PANI and (c) PANI/22% MWCNT nanocomposite films. (a'), (b') and (c') were higher magnification ($\times 10,000$) images of (a), (b) and (c), respectively.

3.2. Electrical Conductivity of the PANI/MWNT Nanocomposites Film

The electrical resistance of the composites were measured because these would be needed to correlate with the strain sensing capability of the composites. The electrical resistance (R) of PANI/11% MWCNT, PANI/22% MWCNT, PANI/44% MWCNT, pure PANI and pure MWCNT films were measured by a multimeter at room temperature. The measure distance between two electrodes for measurement is 1.5 cm. Three samples were measured for each composites films and the mean values and deviations are shown in Fig. 9. It is found that the electrical resistance of pure MWCNT film was 5.9Ω , while the pure PANI film's resistance is 152Ω showing the highest R value compared to the other four films. The resistance of PANI/11% MWCNT was reduced to around 70Ω . Lower resistances were achieved by adding more MWCNT into the composition. The resistance values of PANI/22% MWCNT and PANI/44% MWCNT are about 16.3Ω and 14.6Ω , respectively, which are close. It indicated that the MWCNT network was firmly established when 22% MWCNT was added into the composition and adding more MWCNT would change the conductivity of the composition films marginally.

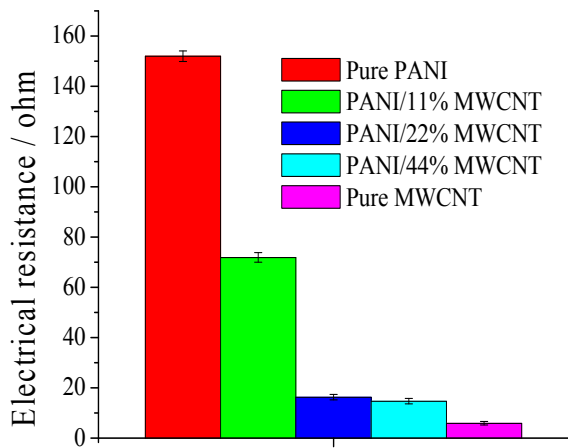


Fig. 9. Electrical conductivity and standard deviations of PANI/11% MWCNT, PANI/22% MWCNT, PANI/44% MWCNT, pure PANI and pure MWCNT films measured by multimeter.

3.3. Mechanical Properties of the PANI/MWNT Nanocomposite Films

A nanoindentation test was used to study the mechanical properties of PANI/22% MWCNT nanocomposite films. Six different locations were randomly selected to do the test. Fig. 10 shows the most typical curve of the test.

The hardness standard deviation of PANI/22% MWCNT nanocomposite films was 0.0066 GPa and the Young's modulus deviation was 0.0803 GPa. This can be explained by the random spaghetti-like arrangement of PANI/MWCNT microstructure that resulted in local porosity and agglomerates. Also, the nanoindentation test results clearly showed that the PANI greatly contributed to increase the Young's modulus and hardness values of the PANI/22% MWCNT nanocomposite films.

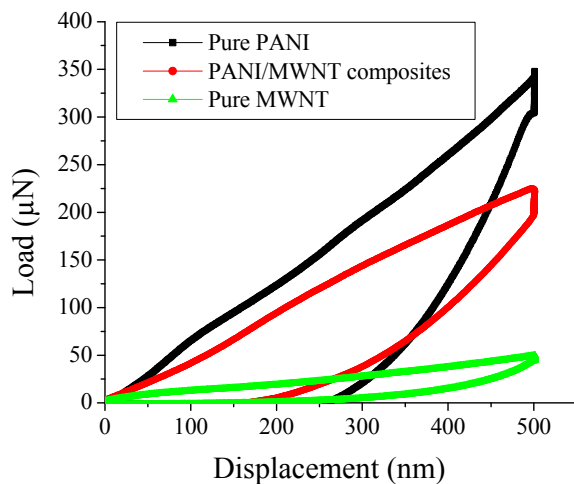
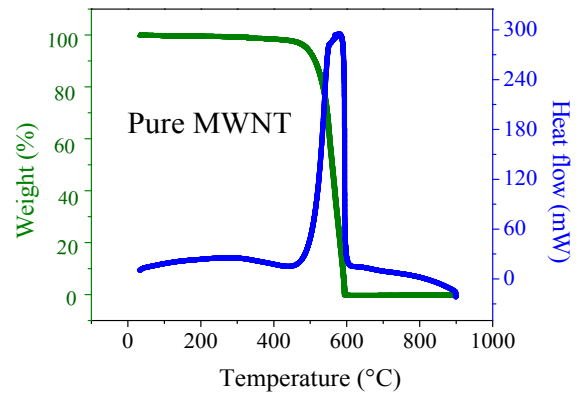


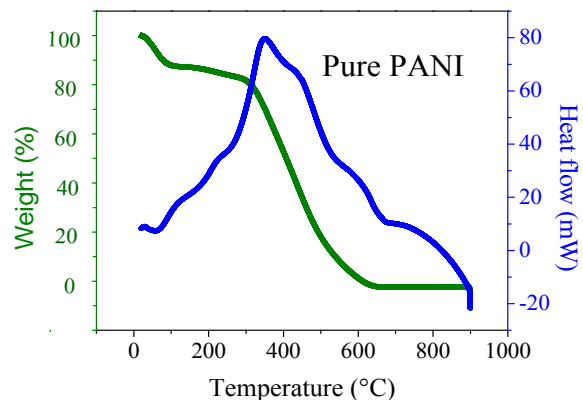
Fig. 10. Nanoindentation (loading–unloading curves) of pristine PANI, pure MWCNT and PANI/22% MWCNT nanocomposite film.

3.4. Thermal Stability of the PANI/MWCNT Nanocomposites Films

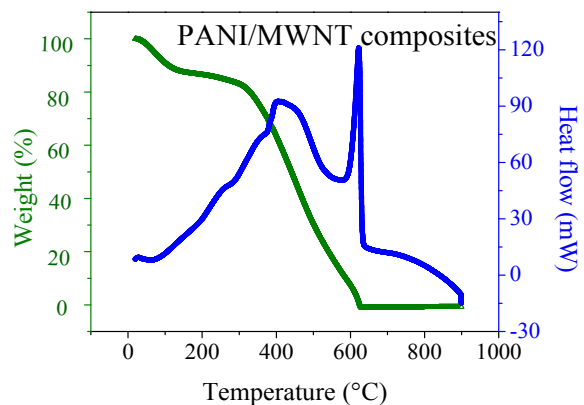
Thermal stability of the composite was evaluated because one of the primary tasks of the sample would be its use in high temperature applications. The results of Simultaneous DSC-TGA (SDT) test in nitrogen are shown in Fig. 11. It could be seen that the pure MWCNT could not be decomposed until the temperatures reached around 550 °C, while the pure PANI started to decompose when the temperature reached 350 °C.



(a)



(b)



(c)

Fig. 11. SDT curve for pristine MWCNT, pure PANI and PANI/22% MWCNT composites films.

There are two major stages of weight loss for the polyaniline, regardless of the experimental environments. The first weight loss occurs at the lower temperature of about 50 °C and results from moisture evaporation and perhaps outgassing of unknown small molecules. The second weight loss indicates a structural decomposition of the polymer and occurs at the higher temperature which starts at about 350 °C.

For PANI/22% MWCNT nanocomposites, there are two strong exothermic peaks at 400 °C and 600 °C, which correspond to the exothermic peak of PANI and MWNT, respectively. It could be easily concluded that the thermal stability of the PANI/22% MWNT was improved by about 50 °C. It also shows two major stages of weight loss in the nanocomposites. The first one is caused by removal of water and small molecules, while the second one is because of the decomposition of MWCNT and PANI.

3.5 Damping Ratios Discussion

As mentioned previously, the reason for the creation of the composite is for use as a sensor-actuator with damping capabilities. To check on the damping capability aspect, several tests were performed. For the first test, free vibration trial results are shown in Fig. 12.

Five trials were run for each of the different composites listed. The tests indicated that the PANI/11 % MWCNT composite displayed higher damping ratios than pure PANI, PANI/22% MWCNT, PANI/44 % MWCNT and pure MWCNT when clamped either close to the uncovered * side or close to the sample # side (see Fig. 5 for locations). The damping ratio of PANI/11 % MWCNT was 1.8 times larger than that of pure PANI and 1.35 times higher than PANI/22% MWCNT when clamped on the uncovered * side. However, the damping ratio of PANI/11 % MWCNT was double that of the pure PANI and 1.43 times more than PANI/22% MWCNT when clamped on the sample # side. Also, when clamped on the sample # side, the damping values were 2.2 to 3.1 times higher for each composite when compared to being clamped on the uncovered * side.

The damping ratio of PANI/11% MWCNT composite was 0.00656 when clamped on the uncovered * side; however, it reached a value of 0.0204 when clamped to the sample # side. Thus, it indicated that where the samples were placed on the base beams played an important role in the damping results. Further, all PANI/MWCNT combinations had damping ratios that were much better than pure MWCNT alone. Our MWCNT damping ratio results were similar to those found by Li and Levy [17].

For the second test (see Fig. 5 for the configuration of the test setup), free vibration test results showed that the damping ratio of the PANI/11% MWCNT sample attached to only one side of Al base beam was 0.00382. However, the damping ratio achieved for the double sided coverage

reached a value of 0.072, which is 18.85 times higher than for the single sided coverage. By comparing the vibration traces shown in the Fig. 13, we note that when the system vibrates from the same starting conditions, the double sided coverage (black trace) attenuates the vibrations in a much shorter period of time than its single sided counterpart. In other words, the damping effect will be dramatically increased when both sides of the Al base beam is covered by PANI/11% MWCNT. This result follows the trends found in Chen and Levy [18] for a constrained double sandwich viscoelastic material covering an Al base beam.

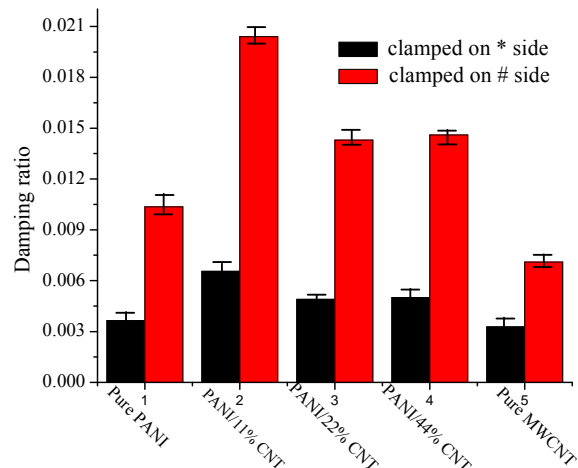


Fig. 12. Damping ratios and standard deviation of rectangular pure PANI, PANI/11% MWCNT, PANI/22% MWCNT, PANI/44% MWCNT and pure MWCNT clamped on the uncovered * side and sample # side.

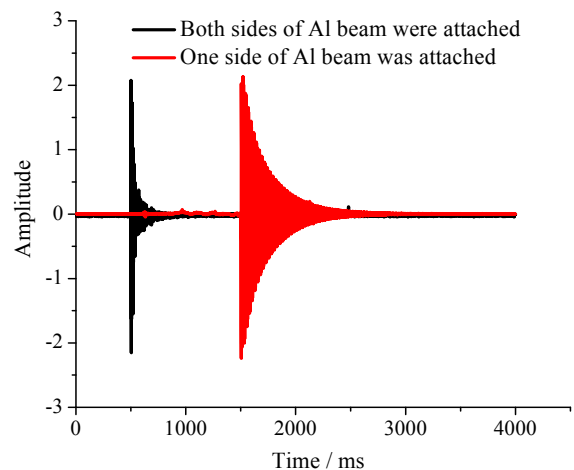


Fig. 13. Comparison of free vibration damping test between PANI/11% MWCNT single side covered (red) and PANI/11% MWCNT double sides covered (black) Al base beam.

Our PANI/MWCNT system was specifically created to replace such a constrained viscoelastic system, saving on weight of the constraining layer and the viscoelastic material, yet still maintaining the

constraining layer stiffness through the MWCNT and introducing damping through the PANI for vibration attenuation.

For the third test (see Fig. 6 for the configuration of the test setup), the width of the PANI/MWCNT sample is 0.8 cm, while the width of the Al beam is 0.9 cm. Thus, 88.89 % Al beam was covered by sample in width direction. From the data shown in Fig. 14, we could see that for 2.4 mm thickness Al beam, the damping ratio was 0.00492 when the beam was clamped at (a) in Fig. 14. The damping ratio increased when the distance between the clamp and the sample was increased. It reached a value of 0.00685 when the distance between the clamps to the sample is 5.4 cm. Then, it decreased to 0.00452 when the distance is 7.7 cm from the clamp to the sample.

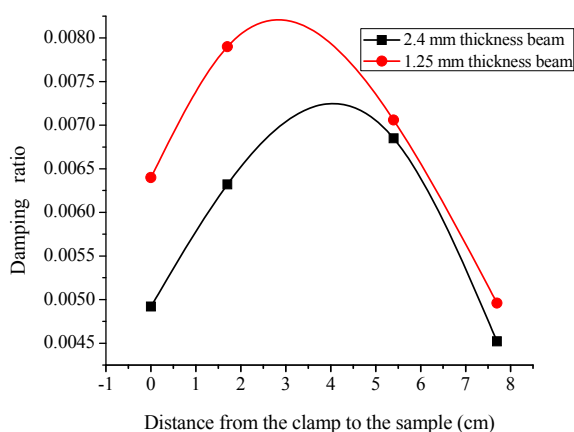


Fig. 14. Damping ratios of 2.4 mm and 1.25 mm thickness Al beams with different distance from the clamped side of the beam to the right end of the sample.

Meanwhile, for 1.25 mm thickness Al beam, the same pattern was deduced as described for the 2.4 mm thick beam but the values were higher. The damping ratio reached 0.0079 when the distance from the clamp to the sample was 1.7 cm. Also, compared with the sample attached onto the thick Al beam, the PANI/MWCNT attached onto the thin Al beam peaked, i.e., had higher damping ratios when the clamped condition occurred closer to the sample (0.0082 at approximately 2.5 cm from the sample vs. 0.0072 at approximately 4 cm from the sample), as shown in Fig. 14.

4. Conclusion

Different compositions of PANI/MWCNT nanocomposites were synthesized through an *in situ* polymerization method. Frit compression method was introduced to make PANI/MWCNT nanocomposite films/discs. SEM and TEM results showed that this technique produced a homogeneous coating of PANI onto the MWCNT, which indicated that carbon nanotubes were well dispersed in the polymer matrix. The electrical resistance was largely

reduced by introducing MWCNT into the PANI. The electrical resistance of the composites could be controlled by adding specific amounts of the MWCNT. Nanoindentation test results showed that the PANI greatly contributed to the increase in the Young's modulus and hardness of the PANI/22% MWCNT nanocomposites films. The results of Simultaneous DSC-TGA (SDT) test indicate that thermal stability of PANI/22% MWCNT was improved by about 50 °C.

Preliminary free vibration tests results showed that PANI/11%MWCNT displayed higher damping ratio than pure PANI, PANI/22%MWCNT, PANI/44%MWCNT and pure MWCNT, meaning that further addition of MWCNT to increase the electrical conductivity of the composite actually reduced the damping capability of the PANI/MWCNT composite. Furthermore, the location of the clamped support of the cantilever beam while performing the free vibration damping tests was very important to the magnitude of the damping ratio. When the beam was clamped close to the sample end, it displayed higher damping ratios than when clamped to the free, uncovered end. Damping test were also run for both single and double sided PANI/11%MWCNT coverage on Al base beam. The results showed that by attaching the nanocomposite sample to both sides of Al beam, the damping ratio reached a value of 0.072, which is 18.85 times higher than for the single sided coverage. Furthermore, the thinner Al base beams were found to have higher damping ratios than the thicker Al base beams. The damping ratios were again found to have a maximum that depended on the amount of coverage of the beam by the sample. These results follow the trends found in Chen and Levy [18, 19] in their discussions of effect of damping coverage length versus system loss factor as well as effect of end mass on system loss factor as a function of coverage length. In certain situations where the weight of the sample is deemed to be a significant fraction of the beam weight, the sample must be treated as an end mass and results must be compared to those of a vibrating beam with an effective end mass. This damping aspect that has been found as well as sample coverage size will be investigated further as its usefulness is very important to vibration attenuation uses of the sample.

Acknowledgement

The authors are grateful to the US Army Research Laboratory and US Army Research Office for the following Grant No. 58940-RT-REP that enabled this work to be possible.

References

- [1]. Kireitseu M., Vibration damping/dynamic properties of CNT-reinforced composite structures, *NSTI-Nanotech*, 2006, 1, pp. 198-201.

- [2]. Hazarika A., Maji T. K., Strain sensing behavior and dynamic mechanical properties of carbon nanotubes/nanoclay reinforced wood polymer nanocomposite. *Chemical Engineering Journal*, 2014, 247, pp. 33–41.
- [3]. Alva A., Raja S., Damping characteristics of epoxy-reinforced composite with multiwall carbon nanotubes, *Mechanics of Advanced Materials and Structures*, 2014, 21, 3, pp. 197-206.
- [4]. Suhr J., Zhang W., Ajayan P M, Koratkar, N A., Temperature-activated interfacial friction damping in carbon nanotube polymer composites, *Nano Letters*, 2006, 6, 2, pp. 219-223.
- [5]. Suhr J., Koratkar N., Effect of pre-strain on interfacial friction damping in carbon nanotube polymer composites, *Journal of Nanoscience and Nanotechnology*, 2006, 2, pp. 483-6.
- [6]. Liu S., Chen F., Zhang Y., Shen Q., Huang Z., Zhang L., Interfacial bond dependence of damping properties of carbon nanotubes enhanced polymers, *Polymer Composites*, 2014, 35, 3, pp. 548-556.
- [7]. Dresselhaus M., Dresselhaus G., Eklund P., Science of fullerenes and carbon nanotubes, *Academic Press*, San Diego, California, USA, 1996.
- [8]. Huang F., Vanhaecke E., Chen D., *In situ* polymerization and characterizations of polyaniline on MWCNT powders and aligned MWCNT films, *Catalysis Today*, 2010, 150, 1-2, pp. 71–76.
- [9]. Qiao Y., Li C.M., Bao S., Bao Q., Carbon nanotube/polyaniline composite as anode material for microbial fuel cells, *Journal of Power Sources*, 2007, 170, 1, pp. 79-84.
- [10]. Wang C., Mottaghitalab V., Too C., Spinks G., Wallaceand G., Polyaniline and polyaniline/carbon nanotube composite fibres as battery materials in ionic liquid electrolyte, *Journal of Power Sources*, 2007, 163, pp. 1105-1109.
- [11]. Lu X., Dou H., Yang S., Hao L., Zhang L., Shen L., et al., Fabrication and electrochemical capacitance of hierarchical graphene/polyaniline/carbon nanotube ternary composite film, *Electrochimica Acta*, 2011, 56, 25, pp. 9224–9232.
- [12]. Meng C., Liu C., Fan S., Flexible carbon nanotube/polyaniline paper-like films and their enhanced electrochemical properties, *Electrochemistry Communications*, 2009, 11, pp. 186–189.
- [13]. http://en.wikipedia.org/wiki/Frit_compression (Last Accessed Nov 4, 2014).
- [14]. Whitby R. L. D., Fukuda T., Maekawa T., James S. L., Mikhailovsky S. V., Geometric control and tuneable pore size distribution of buckypaper and buckydiscs, *Carbon*, 2008, 46, 6, pp. 949-956.
- [15]. <http://www.nano-lab.com/buckypaper.html> (Last Accessed November 4, 2014).
- [16]. Tasis D., Tagmatarchis N., Bianco A., Prato M., Chemistry of carbon nanotubes, *Chemical Reviews*, 2006, 106, 3, pp. 1105–1136.
- [17]. Li, X., and Levy, C., A Novel Strain Gauge with Damping Capability, *Sensors & Transducers*, Special Issue, 2009, 7, 10, pp. 5-14.
- [18]. Chen Q., Levy C., Vibration Analysis of a Partially Covered, Double Sandwich Cantilever Beam with Concentrated Mass at the Free End, *International Journal of Solids and Structures*, 1994, 31, pp. 2377-2391.
- [19]. Chen Q., Levy C., Vibration Characteristics of a Partially Covered Double Sandwich Cantilever Beam, *AIAA Journal*, 1996, 34, pp. 2622-2626.

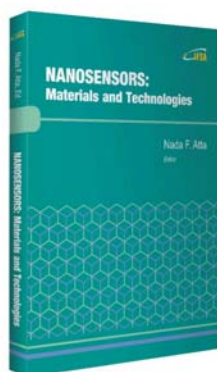
2015 Copyright ©, International Frequency Sensor Association (IFSA) Publishing, S. L. All rights reserved. (<http://www.sensorsportal.com>)

NANOSENSORS: Materials and Technologies

Hardcover: ISBN 978-84-616-5378-2
e-Book: ISBN 978-84-616-5422-2



Nada F. Atta, Ed.



Nanosensors: Materials and Technologies aims to provide the readers with some of the most recent development of new and advanced materials such as carbon nanotubes, graphene, sol-gel films, self-assembly layers in presence of surface active agents, nano-particles, and conducting polymers in the surface structuring for sensing applications. The emphasis of the presentations is devoted to the difference in properties and its relation to the mechanism of detection and specificity. Miniaturization on the other hand, is of unique importance for sensors applications. The chapters of this book present the usage of robust, small, sensitive and reliable sensors that take advantage of the growing interest in nano-structures. Different chemical species are taken as good example of the determination of different chemical substances industrially, medically and environmentally. A separate chapter in this book will be devoted to molecular recognition using surface templating.

The present book will find a large audience of specialists and scientists or engineers working in the area of sensors and its technological applications. The *Nanosensors: Materials and Technologies* will also be useful for researchers working in the field of electrochemical and biosensors since it presents a collection of achievements in different areas of sensors applications.

Order: http://www.sensorsportal.com/HTML/BOOKSTORE/Nanosensors_IFSA.htm